(12)

David Taylor Research Center

Bethesda, Maryland 20084-5000

Carderock Div/SHD-1387-02 December 1992

Ship Hydromechanics Department

THRUST DEDUCTION PREDICTION FOR HIGH SPEED COMBATANT SHIP

By

Yoon-Ho Kim

Approved for Public Release, Distribution Unlimited

UNCLASSIFIED
SECURITY CLASSIFICATION OF THIS PAGE

REPORT DOCUMENTATION PAGE

1a REPORT SECURITY CLASSIFICATION UNCLASSIFIED	1b RESTRICTIVE MARKINGS
2a SECURITY CLASSIFICATION AUTHORITY	3 DISTRIBUTION / AVAILABILITY OF REPORT Approved for Public Release; Distribution Unlimited
2b DECLASSIFICATION / DOWNGRADING SCHEDULE	
4 PERFORMING ORGANIZATION REPORT NUMBER(S) Carderock Div/SHD 1387-02	5 MONITORING ORGANIZATION REPORT NUMBER(S)
6a NAME OF PERFORMING ORGANIZATION David Taylor Model Basin Carderock Division NSWC 6b OFFICE SYMBOL (If applicable)	7a. NAME OF MONITORING ORGANIZATION
6c ADDRESS (City, State, and ZIP Code) Bethesda, MD 20084-5000	7b. ADDRESS (City, State, and ZIP Code)
8a NAME OF FUNDING / SPONSORING ORGANIZATION Naval Sea Systems Command 8b. OFFICE SYMBOL (If applicable) 05Z	9. PROCUREMENT INSTRUMENT IDENTIFICATION NUMBER
8c ADDRESS (City, State, and ZIP Code) Washington, D.C. 20362-5101	10 SOURCE OF FUNDING NUMBERS PROGRAM ELEMENT NO. 63573N PROJECT NO TASK NO. WORK UNIT ACCESSION NO 1-2700-724

11 TITLE (Include Security Classification)
Thrust Deduction Prediction for High Speed Combatant Ship

12 PERSONAL AUTHOR(S)
Yoon-Ho Kim

13a TYPE OF REPORT	13b TIME COVERED	14. DATE OF REPORT (Year, Month, Day)	15 PAGE COUNT
Final	FROM ____ TO ____	1992, December	23+v

16 SUPPLEMENTARY NOTATION

17 COSATI CODES			18. SUBJECT TERMS (Continue on reverse if necessary and identify by block number)
FIELD	GROUP	SUB-GROUP	Resistance, Actuator Disk, Powering, Thrust, Panel Method

19 ABSTRACT (Continue on reverse if necessary and identify by block number)

The free surface effects on the hull-propeller interaction characteristic of thrust deduction have been studied for a high speed combatant ship hull form. Through mathematical modelling and a series of numerical computations, we attempt to elucidate the mechanism of this component of hull-propeller interaction from the free surface. SWIFT, a linearized free surface potential flow solver using a higher-order panel method, has been extended to study the interaction between the double hull and propeller as well as the hull-propeller interaction under free surface waves. The propeller is simulated using an actuator disk. Thrust loading coefficients from propeller open-water tests provide the sink strength for the disk. This ship has inclined propeller shafts and the measured wakes at the propeller plane clearly indicate that the propellers are operating outside the turbulent boundary layer at the ship stern. The viscous effects are not treated here. The pressure on the hull is integrated to obtain the resistance for the double body flow with/without propellers, and also for the body and free surface flow with/without propellers. The computed thrust deduction fractions show good agreement with the experimental data. For this particular ship, the free surface wave effect on thrust deduction is not small and lies between 25% to 30% of the total, depending upon speeds.

20 DISTRIBUTION / AVAILABILITY OF ABSTRACT ☒ UNCLASSIFIED/UNLIMITED ☐ SAME AS RPT ☐ DTIC USERS	21 ABSTRACT SECURITY CLASSIFICATION UNCLASSIFIED
22a NAME OF RESPONSIBLE INDIVIDUAL Yoon-HO Kim	22b TELEPHONE (Include Area Code) (301) 227-1594 22c OFFICE SYMBOL code 1522

DD FORM 1473, 84 MAR 83 APR edition may be used until exhausted
All other editions are obsolete

SECURITY CLASSIFICATION OF THIS PAGE

CONTENTS

FIGURES

TABLES

NOMENCLATURE

A_O	Propeller disk area, $A_O = \pi(R_p^2 - R_h^2)$
C_D	Drag coefficient, $C_D = D/\left(\frac{1}{2}\rho U^2 A_o\right)$
C_P	Pressure coefficient, C_P = Pressure$/\left(\frac{1}{2}\rho U^2\right)$
C_R	Resistance coefficient, C_R = Resistance$/\left(\frac{1}{2}\rho U^2 S\right)$
C_{TH}	Thrust loading coefficient, $C_{TH} = T/\left(\frac{1}{2}\rho A_o U^2\right)$
D	Drag augmentation, D = T - R
g	Gravitational acceleration
h	Transom stern depth measured from undisturbed free surface to bottom edge
q	Sink strength at an actuator disk
R	Barehull Resistance
Rp	Propeller tip radius
R_h	Propeller hub radius
S	Ship wetted surface
T	Propeller thrust
t	Thrust deduction fraction
t_p, t_v, t_w	Thrust deduction fraction due to double body potential, viscous, and free-surface wave, respectively
U	Ship speed
v	Perturbed velocity
V	Total velocity, V=U+v
V_A	Speed of advance of the propeller
w	Wake
w_E	Effective wake
w_p, w_v, w_w	Wake due to double body potential, viscous, free surface wave, respectively
w_T	Taylor wake fraction, determined by measurement in a powering experiment
x,y,z	Cartesian coordinate system fixed on the ship
Φ	Total velocity potential
ϕ	Perturbed velocity potential
$\phi_{db}, \phi_h, \phi_w$	Velocity potential for double body, ship, and free surface, respectively
ψ_p	Velocity potential due to propeller
ρ	Fluid density
$\sigma(\xi,\eta)$	Source strength distribution across a panel
ξ,η,ζ	Local coordinate system

ABSTRACT

The free surface effects on the hull-propeller interaction characteristic of thrust deduction have been studied for a high speed combatant ship hull form. Through mathematical modelling and a series of numerical computations, we attempt to elucidate the mechanism of this component of hull-propeller interaction from the free surface. SWIFT, a linearized free surface potential flow solver using a higher-order panel method, has been extended to study the interaction between the double hull and propeller as well as the hull-propeller interaction under free surface waves. The propeller is simulated using an actuator disk. Thrust loading coefficients from propeller open-water tests provide the sink strength for the disk. This ship has inclined propeller shafts and the measured wakes at the propeller plane clearly indicate that the propellers are operating outside the turbulent boundary layer at the ship stern. The viscous effects are not treated here. The pressure on the hull is integrated to obtain the resistance for the double body flow with/without propellers, and also for the body and free surface flow with/without propellers. The computed thrust deduction fractions show good agreement with the experimental data. For this particular ship, the free surface wave effect on thrust deduction is not small and lies between 25% to 30% of the total, depending upon speeds.

ADMINISTRATIVE INFORMATION

This work was funded by the Naval Sea Systems Command, Advanced Surface Machinery Systems Program Office, NAVSEA 05Z, under Program Element 63573N. This work was coordinated by the David Taylor Model Basin(DTMB) Program Office of the Advanced Surface Machinery Systems Program, Code 2713, and by the Advanced Propulsor Program Office, Code 1508. It was performed at DTMB, Carderock Division Headquarters,Naval Surface Warfare Center(CDNSWC), where it is identified by Work Unit No. 1-2700-724.

INTRODUCTION

When two bodies in close proximity to each other move in a fluid there are interaction effects which cause additional forces and moments to be experienced by each body. The additional force arising from propeller-hull interaction is well known to naval architects. A propeller operating at the ship stern accelerates the local flow over the stern of the ship and results in changing pressure distribution which has effect on the hull drag. This change in drag of the hull is called drag augmentation and is expressed in terms of the thrust deduction. The flow acceleration also increases the wall shear stress, and hence, the frictional drag. The flow interactions have important consequences to the engineering estimates of speed and power for the ships. For instance, flow-related features such as propeller proximity to the hull, local hull shape, overall body flow, and the free surface influence are all involved with determining net thrust required and understanding the propulsor-induced drag penalty. Details and order of magnitude estimates are needed for preliminary design studies. Our efforts are concentrated on clarifying the quantitative role of wavemaking due to the presence of the free surface in the phenomenon of hull-propulsor interaction and consequently its contribution to the hydrodynamic propulsive efficiency of the hull-propulsor system.

The interaction may be conveniently studied in terms of propulsion factors, including wake and thrust deduction fraction. The wake w caused by the presence of the hull and the free surface

is a simple measure of the change in propulsor inflow as compared to an equivalent open-water condition, and is defined as follows:

$$w = 1 - \frac{V_A}{U} \tag{1}$$

where U is the ship speed and V_A is the speed of advance of the propeller.

The thrust deduction fraction t is an indirect expression of the fact that the force of resistance acting on the hull is modified as a result of propeller action and is defined as follows:

$$t = \frac{T - R}{T} \tag{2}$$

where R is the barehull resistance and T is the propeller thrust. Following Dickmann's pioneering work[1], the hull-propulsor interaction has been customarily considered as a superposition of three basic effects: zero-Froude-number potential effects, viscous effects, and wave effects due to the presence of the free surface. Using standard notations, wake and thrust deduction fractions are expressed as

$$w = w_p + w_v + w_w \tag{3}$$

$$t = t_p + t_v + t_w \tag{4}$$

where the subscripts p, v, and w denote potential, viscous, and free surface wave, respectively.

Since Dickmann[1], considerable effort has been made to study the potential and viscous effects in hull propeller interaction (see the comprehensive bibliography by Nowacki and Sharma[2]). Beveridge[3] was the first to apply a panel method to represent the practical three-dimensional body and to distribute Rankine type sources across each panel to calculate the flow. He used a constant strength sink disk for the propeller and later introduced a sink disk with radially varying strength derived from propeller lifting-line theory for contrarotating propellers. He computed thrust deduction using Lagally's theorem and the results showed good agreement with the experimental data. Stern et al[4] described a comprehensive viscous-flow method for the computation of propeller-hull interaction in which a numerical method for calculating the viscous flow over the stern and in the wake of a ship is coupled with a propeller-performance in an interactive and iterative manner to predict the combined flow field. In their computation the free surface effect was not included and furthermore a propeller is represented approximately by its induced velocity effects. Therefore, for specified propeller geometry, operating condition, and nonuniform inflow-velocity distribution, the propeller induced effects are assumed known.

Nowacki-Sharma[2] investigated the wave effects due to the presence of the free surface both experimentally and analytically. Thin ship theory was used to compute wave-making resistance. The propeller induced flow was approximated by distributing Havelock source on the actuator disk. They showed that the free surface wave component can be dominant in the wake and quite significant in the thrust deduction at some Froude numbers. Yamazaki-Nakatake[5] conducted experiments using the similar mathematical hull of Nowacki-Sharma. They used a different model propeller, but kept the same propeller-diameter to the ship-draft ratio. With careful and systematic series of experiments they observed that the thrust deduction fraction generally

varies with the extent of wave making. All the studies showed that the wave making effect on the thrust deduction is not small, even at high speed.

The wake fraction for high speed combatant ships is known experimentally to be small, usually between ±0.02, while the wake fraction for single screw commercial ships varies from 0.2 for low block to 0.5 for high block coefficient ship. The ship hull we consider in this study is a high speed, transom stern ship. The measured wake fraction in the propeller plane for this model ranges from 0.01 to 0.04 depending upon the speeds. A panel method is employed for this study. The zero-Froude-number potential effects are computed first. Next when we consider the free surface wave effects, the body boundary condition has been modified at the transom stern. In the following, we briefly outline the numerical approach and the computed results are discussed along with the measurements.

NUMERICAL APPROACH

Suppose that a ship moves in the positive x-direction with constant forward speed U in calm water. A Cartesian coordinate system $x_i = (x,y,z)$ translates with the ship as shown in Fig. 1. The z=0 plane is taken as the undisturbed free surface, the positive x-axis in the direction of the ship's forward velocity, and the positive z-axis upward. The boundary-value problem will be expressed relative to this moving coordinate system with the flow at infinity consisting of an uniform stream. The fluid is assumed to be inviscid and incompressible and its motion is irrotational such that the velocity field of the fluid can be defined as

$$\vec{v}(x,y,z) = \nabla\phi(x,y,z) \tag{5}$$

where $\phi(x,y,z)$ is the velocity potential and satisfies the Laplace equation

$$\nabla^2\phi = 0 \tag{6}$$

in the fluid domain D and the body boundary condition

$$\nabla\phi\cdot\vec{n} = \vec{U}\cdot\vec{n} \tag{7}$$

on the body surface S_B where $n = (n_x, n_y, n_z)$ denotes the outward unit normal vector on the boundary. Furthermore the disturbance due to free surface is assumed to be sufficiently small that the nonlinear free surface condition may be linearized.

$$U^2\phi_{xx} + g\phi_z = 0. \qquad \text{at } z=0 \tag{8}$$

Energy conservation requires that velocity potential approach the uniform onset flow potential and that there be no waves far upstream of the ship, and that waves always travel downstream.

There are two common approaches to solve this boundary value problem: Havelock source and Rankine type singularity distribution methods. Havelock source has been developed to satisfy the linearized free surface and radiation conditions. But, because of its complex kernel function, its application to practical hull configurations is much more difficult and cumbersome. Rankine type

singularity, on the other hand, has simple kernel function and is easier for handling the details of complex hull geometry. The geometry of ship stern fitted with propulsion system is particularly complicated and a boundary element method may be the only method capable to handle the details of its complex configuration with sufficient accuracy. A well-known drawback of this approach is the necessity of proper numerical implementation of the radiation condition for free surface waves. Dawson[6] successfully introduced an upstream finite difference operator to Rankine method when implementing the free surface condition in order to satisfy the radiation condition.

The method adopted here is a boundary element method. The ship hull, propeller, and free surface are discretized into many small quadrilaterals. Across each quadrilateral the Rankine source($1/r$) is distributed. The source strength σ at a point (ξ,η,ζ) is assumed to vary linearly across the quadrilateral

$$\sigma(\xi,\eta) = \sigma_o + \sigma_\xi \xi + \sigma_\eta \eta . \tag{9}$$

The coefficients in Eq. (9) are determined by using a method of weighted squares over the panel and up to eight of its neighboring panels. This method requires that the form of Eq. (9) give exactly the singularity value at its centroid and approximate values in the least square sense at centroid of the neighboring panels. We used curved panels to patch the ship and free surface. Each quadrilateral may be represented in the approximate form

$$\zeta(\xi,\eta) = \zeta_o + \zeta_\xi \xi + \zeta_\eta \eta + \frac{1}{2}\zeta_{\xi\xi}\xi^2 + \zeta_{\xi\eta}\xi\eta + \frac{1}{2}\zeta_{\eta\eta}\eta^2 \tag{10}$$

where (ξ,η,ζ) are orthogonal coordinates local to S. The six coefficients in Eq.(10) are determined by requiring that the approximate surface given by Eq. (10) pass through its four corner points exactly and through its neighboring points approximately in a least square sense. The boundary-value problem formulated above then reduces to a determination of an unknown singularity distribution over the boundary surface of the fluid domain.

We linearized the boundary value problem and hence the velocity potential ϕ can be assumed linear superposition of each disturbance. In case of a double body model without propeller $\phi = \phi_{db}$, a double body with propeller $\phi = \phi_{db}+\phi_p$, a towed ship without propeller $\phi = \phi_h+\phi_w$, and a self-propelling ship $\phi = \phi_h+\phi_w+\phi_\eta$. In the following, each velocity potential will be discussed first and components of thrust deduction fraction t_p and t_w will be considered next.

Ship Hull

The velocity potential induced by the Rankine source distribution on the hull surface may be given by

$$\phi_h = -\frac{1}{4\pi}\int_{S_B} \frac{\sigma}{r} ds \tag{11}$$

or for a double body model case

$$\phi_{db} = -\frac{1}{4\pi}\int_{S_B} \sigma\left(\frac{1}{r}+\frac{1}{r'}\right) ds \tag{11}'$$

where $r = ((x-\xi)^2+(y-\eta)^2+(z-\zeta)^2)^{1/2}$, $r' = ((x-\xi)^2+(y-\eta)^2+(z+\zeta)^2)^{1/2}$, σ the unknown source strength, and S_B the wetted hull surface. If we discretize the hull into N_B number of panels, then the velocity potential can be expressed as follows:

$$\phi_h = -\frac{1}{4\pi}\sum_{i=1}^{N_B}\left(\int_{S_i}\frac{\sigma}{r}ds\right) \tag{12}$$

or

$$\phi_h = -\frac{1}{4\pi}\sum_{i=1}^{N_B}\left(\int_{S_i}\sigma\left(\frac{1}{r}+\frac{1}{r'}\right)ds\right) \tag{12}'$$

The unknown singularity strength distribution σ is determined by satisfying the body boundary condition (7).

Propeller

Following Dickmann[1], the propeller is modelled by a sin-flow actuator disk. Similar to Eq.(11) the propeller induced velocity potential may be expressed as

$$\phi_p = \frac{1}{4\pi}\int_{S_p}\frac{q}{r}ds = \frac{q}{4\pi}\sum_{i=1}^{N_p}\left(\int_{S_i}\frac{1}{r}ds\right) \tag{13}$$

where N_p is the total number of panels used to represent the propeller. In case of a double body model, we use z=0 as a plane of symmetry and have a similar expression of Eqs. (11)' and (12)'. Unknown sink strength q is assumed constant. Propeller loading is incorporated when determining unknown sink strength distribution q across the disk as follows:

$$q = (1-w_E) - \sqrt{(1-w_E)^2+C_{TH}} \tag{14}$$

where w_E is the measured effective wake fraction. The thrust loading coefficient C_{TH} is customarily given as

$$C_{TH} = \frac{T}{\frac{1}{2}\rho A_o U^2} \tag{15}$$

where ρ is the water density, $A_0 = \pi(R_p^2-R_h^2)$ the propeller disk area in which R_p and R_h are the propeller tip and the propeller hub radius, respectively. The drag augmentation D is the difference between the thrust and the resistance, i.e., D = T-R and its coefficient is defined by

$$C_D = \frac{D}{\frac{1}{2}\rho A_o U^2} \tag{16}$$

From Eqs. (2), (15), and (16) the thrust deduction fraction t can be expressed as follows:

$$t = \frac{T-R}{T} = \frac{D}{T} = \frac{C_D}{C_{TH}}. \tag{17}$$

Free Surface Wave

The velocity potential due to the presence of the free surface has the similar expression of Eqs.(11) and (12), i.e.,

$$\phi_w = -\frac{1}{4\pi}\int_{S_w} \frac{\sigma}{r} ds = -\frac{1}{4\pi}\sum_{i=1}^{N_w}\left(\int_{S_i} \frac{\sigma}{r} ds\right) \tag{18}$$

Here infinite free surface domain is truncated into the finite domain S_W for computational reason, and N_W is the total number of panels used to represent the truncated free surface domain.

DDG 51 hull has transom stern. During the model experiment we observed that at ship speed greater than 20 knots the flow clears the stern completely and the cross section becomes dry. In order to model this physical phenomena numerically, we impose two conditions at the stern. First, to satisfy the dry condition at the cross section of the transom stern, we do not put any panels to represent the cross section and leave it empty, in other words, the ship hull is not closed at the stern. Secondly, at the bottom edge of the transom stern, the body boundary condition of Eq.(7) is replaced by the requirement that the flow pass by each bottom edge panel tangentially. The magnitude of the tangential velocity is assumed equal to square root of the hydrostatic term 2gh of Bernoulli equation

$$\frac{p}{\rho} + \frac{V^2}{2} + gh = \frac{p_o}{\rho} + \frac{U^2}{2} \tag{19}$$

in which p_0 is the atmospheric pressure, $\vec{V} = \vec{U} + \vec{v}$, g is the gravitational acceleration, and h is the depth of the transom stern measured from the undisturbed free surface to the bottom edge. The angle of tangential velocity is obtained by extrapolating values from neighboring panels at the bottom edge of transom stern.

A computer code named SWIFT(Surface Wave Inviscid Flow Theory), using a higher order panel method, has been developed by Kim et al.[7] to solve the surface ship problem with the linearized free surface condition. Numerous computed results demonstrate its capability to accurately predict the flow field, wave profiles, and wave-making resistance for cruiser stern as well as transom stern type ships. The SWIFT computer code has been used extensively for this study.

COMPONENTS OF THRUST DEDUCTION

Double Model Potential Fraction

The velocity potential for the double body model $\phi = \phi_{db}$ of (11)' satisfies the Laplace equation (6) automatically and unknown singularity strength σ at each panel can be determined by satisfying the body boundary condition (7). Once the singularity distributions are determined as the solution of the boundary-value problem, the velocity potential can be obtained using Eq.(11)' at any point in the fluid domain and the velocity field is determined from Eq.(5). The hydrodynamic pressure coefficient is given by Bernoulli equation(19):

$$C_P = \frac{P}{\frac{1}{2}\rho U^2} = 1 - \frac{V^2}{U^2} \tag{20}$$

and the resistance coefficient C_R can be computed by integrating the pressure over the wetted hull surface

$$C_R = \frac{1}{S_B} \int_{S_B} C_p n_x \, ds \tag{21}$$

In case of a double body model fitted with propeller(s), the total velocity potential ϕ consists of two terms, ϕ_{db} and ϕ_p. The presence of propeller(s) must be taken into account when satisfying the body condition (7) to determine the strength of singularities distributed on the hull. The body boundary condition accordingly becomes

$$\nabla\phi_{db} \cdot \vec{n} = -Un_x - \nabla\phi_p \cdot \vec{n} \qquad \text{on } S_B \tag{22}$$

Again after determining the singularity strength distribution σ on the hull, we compute the velocity distribution on the body from Eq.(5), the pressure distribution from Eq.(20), and finally the resistance coefficient from Eq.(21). The potential fraction t_p is then obtained from

$$t_p = \frac{(C_R^{db})_{w/Prop} - (C_R^{db})_{w/o\ Prop}}{C_{TH}} \tag{23}$$

where $(C_R^{db})_{w/Prop}$ and $(C_R^{db})_{w/o\ Prop}$ are the double body resistance coefficients with and without operating propeller(s), respectively.

Free Surface Wave Fraction

The velocity potential for a towed ship may be expressed as $\phi = \phi_h + \phi_w$. Unknown σ's are determined by satisfying both body boundary condition (7) and free surface condition (8).

Figure 2 shows the typical panel network used for the computation. For a self-propelling ship, the total velocity potential ϕ consists of three components: ϕ_h, ϕ_w, and ϕ_p. Here ϕ_p is assumed known. To determine the singularity strength distribution σ the boundary conditions have to change accordingly, and the body boundary condition becomes

$$\nabla(\phi_h + \phi_w)\cdot\vec{n} = -Un_x - \nabla\phi\cdot\vec{n} \qquad \text{on } S_B$$

and the free surface condition becomes

$$U^2(\phi_h + \phi_w)_{xx} + g(\phi_h + \phi_w)_z = -U^2(\phi_p)_{xx} - g(\phi_p)_z \quad \text{on } z=0$$

After determining σ, computations of velocity potential and velocity field as well as pressure and resistance are straightforward, and the desired wave fraction t_w is obtained as follows:

$$t_w = \frac{(C_R^{h,w})_{w/Prop} - (C_R^{h,w})_{w/o\ Prop}}{C_{TH}} \qquad (24)$$

where $(C_R^{h,w})_{w/Prop}$ and $(C_R^{h,w})_{w/o\ Prop}$ are the resistance coefficients when a ship is moving in calm water with and without operating propeller(s), respectively.

DESCRIPTION OF MODEL

Table 1 shows the particulars of the ship hull. All the quantities are nondimensionalized. A dome is installed at the bow and the stern type is transom. The propeller shaft is inclined 4.5 degree with respect to the keel line. Figure 3 is a schematic drawing of the propeller location, tip radius, and the hub radius. All the model experiments were conducted in the deep water towing tank of David Taylor Model Basin in Carderock Division, NSWC, following standard test procedures for barehull resistance test, wake measurements in the propeller plane, propeller performance tests in open water, and self-propulsion tests. Borda* reported the details of experimental procedures and the results.

RESULTS AND DISCUSSION

Figure 4 shows the discretized ship hull. 320 panels were used to approximate one side of the ship hull surface: 28x8=224 panels for main hull and 12x8=96 panels for bow dome. Using a double body model we examine how the actuator disk model influences the local flow characteristics. Figure 5 shows the computed wake in terms of cross flow velocity vectors at the port side of double body model at Froude number 0.414. All length scales are nondimensionalized by half ship length($L_{pp}/2.0$). The propeller radius R_p becomes 0.03648 and the hub radius R_h is 0.01028. The port side propeller is located at P(x,y,z)= (-0.89178,-0.06,-0.07506). The velocities are computed at four different cross planes situated at x= -0.8188, -0.8553, -0.8735, and -0.8845 and these x-coordinates are equivalent to $2.0*R_p$, $1.0*R_p$, $0.5*R_p$, and $0.2*R_p$ distance away (upstream) from the actuator disk. At each cross plane, 4 different radii: $r=1.1*R_p$, $1.0*R_p$, $0.7*R_p$, and $0.5*R_p$ are considered and at each radius the velocity components V_x,V_y, and V_z are computed at 24 points equally divided along the circumference. Figure 5 has a pair of arrow plots:

* Borda, Gary C., David Taylor Model Basin, CDNSWC, in a document of higher classification

one with and the other without an actuator disk. As shown in Figure 5, the differences in magnitude and direction between each pair become significant as the local flow approaches the actuator disk.

In Table 2, the axial and total velocities are compared between with and without an operating propeller.The values of each velocity are obtained by arithmetic mean at each cross section. Without operating propeller both axial and total velocities decrease their magnitudes progressivley along the x axis. An operating propeller accelerates local flow and the flow speed increases as it approaches to the propeller. The computed results show about 5.5% increment in speed at the cross section x= -0.8845.

786 panels were used to cover the free surface domain: 58x12=696 panels for the main portion of the free surface and 15x6=90 panels for the free surface following the transom stern.The total 1106 panels were used to represent one side of the plane of symmetry.

Model experiments were conducted at Froude number ranging from 0.138 to 0.440 and the wave-making resistances were obtained from the wave cut measurement. In Figure 6, the computed wave-making resistances are compared with the measurements. At Froude number higher than 0.276 the computed results show good agreement with the measurements, but at Froude number lower than 0.276 some difference is noticeable. As mentioned in free surface part of numerical approach, the transom stern was wet until the model reached the Froude number 0.276. We are interested in ship performance at high speeds, and assumed dry transom stern in computation throughout the considered Froude number range.

In Table 3, the computed potential fractions for a double body model are given at four Froude numbers; 0.276, 0.3447, 0.414, and 0.44. It is well known from D'Alambert's paradox that the resistance of a body in unbounded potential flow has to be zero. The non-zero resistance coefficient 0.10452×10^{-3} without propeller comes from the fact that, as discussed in the free surface part of numerical approach, the double body is not closed completely at the stern and left open intentionally to accommodate dry transom stern condition. The computed results show that the contribution of potential fraction to the total thrust deduction fraction is 51% at F_n=0.276, and increases as speed increases, and becomes 66% at F_n=0.44.

Table 4 shows the contribution due to the free surface wave fraction. About 30% contribution is observed at F_n=0.276 and 0.3447, 25% at F_n=0.414, and 26% at F_n=0.44. Table 5 summarizes the thrust deduction fractions obtained from the self-propulsion model experiments and from the computed potential and wave fractions. The experimental t values include all three components; potential(t_p), viscous(t_v), and free-surface wave(t_w), but the computations are limited to estimates of t_p and t_w. The following observations can be made:

(1)At the F_n's between 0.276 and 0.440, the computed t_p+t_w values lie between 80% and 92% of the measured thrust deduction. The difference may be caused by the neglected viscosity effect, or by the limits of computational accuracy and capability, or both.

(2) The component t_w has been customarily neglected because of the numerical difficulties involved in handling the free surface condition and/or because it was thought small quantity. The computational results indicate that for this particular model the t_w term is not small, between 25 and 30% of the measured t, and should not neglect.

(3) The measured wakes lie between 0.01 and 0.04 at the considered speeds. These values are extremely small compared with those values of 0.2 and 0.5 which are common in typical low and high block coefficient commercial ships, respectively. For this ship fitted with the inclined propeller shaft with respect to the keel line the measured values indicate that the propeller plane seems completely outside of the developed hull boundary layer.

(4) The thrust deduction fractions are also sensitive to hull forms. The measured t values for a cruiser stern type ship reported in [2] and [5] varies between 0.1 and 0.3 while those are between 0.07 and 0.095 for this transom stern ship.

CONCLUSIONS AND RECOMMENDATIONS

From the comparisons between the experimental and the computed results, it has been demonstrated that the panel method is capable of handling an important practical hull configuration and can provide reasonable qualitative and quantitative results for the potential and free-surface wave components of thrust deduction. Thus far the present panel method approach for the calculation of the free surface effect on thrust deduction has been applied in detail to this one example case. Though the viscous effects are not considered here, a method is now in hand to make estimate of the effect of the free surface waves on the thrust deduction fraction. With regard to these quantitative results, the following general comments apply:

- Over the speed range of the ship, the free surface wave component of thrust deduction, t_w, is not negligibly small.
- For a transom stern ship with some inclined propeller shaft angle, the measured onset flow to the propeller seems essentially uniform. The propeller disk is lying outside the hull wake shadow and the viscous fraction t_v is expected small.
- To improve the prediction of the local propeiler-induced flow field, the simple actuator disk model with constant sink strength must be replaced with a more accurate propeller model which could include the effect of onset flow inclination as well.

ACKNOWLEDGMENTS

The author expresses his gratitude to Dr. M.B. Wilson and Dr. K.H. Kim for their valuable suggestions and support.

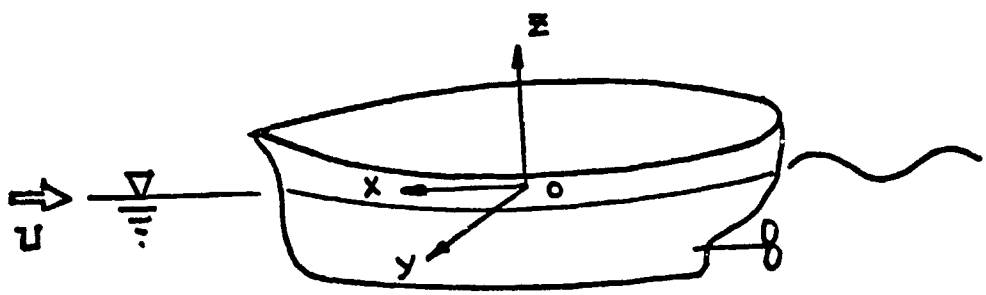

Figure 1. Coordinate System

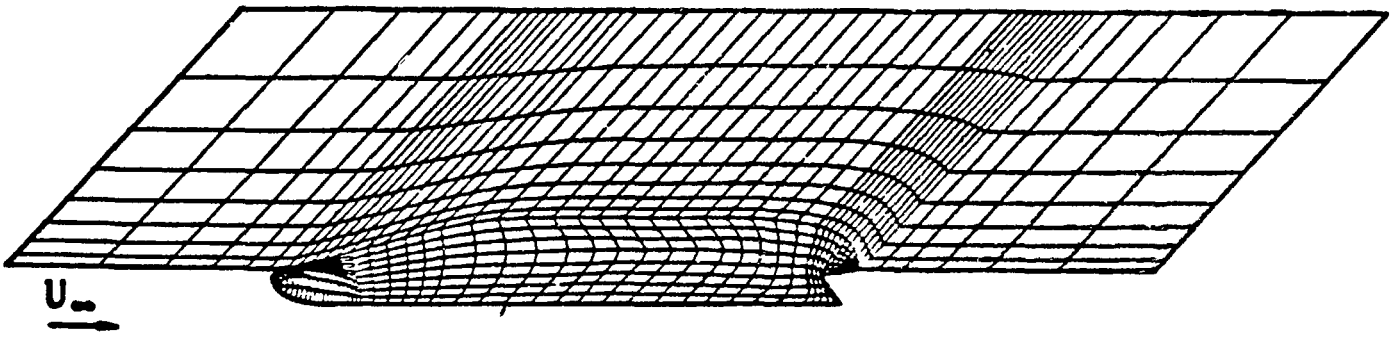

Figure 2. Typical Panel Arrangement for a Ship and Free Surface

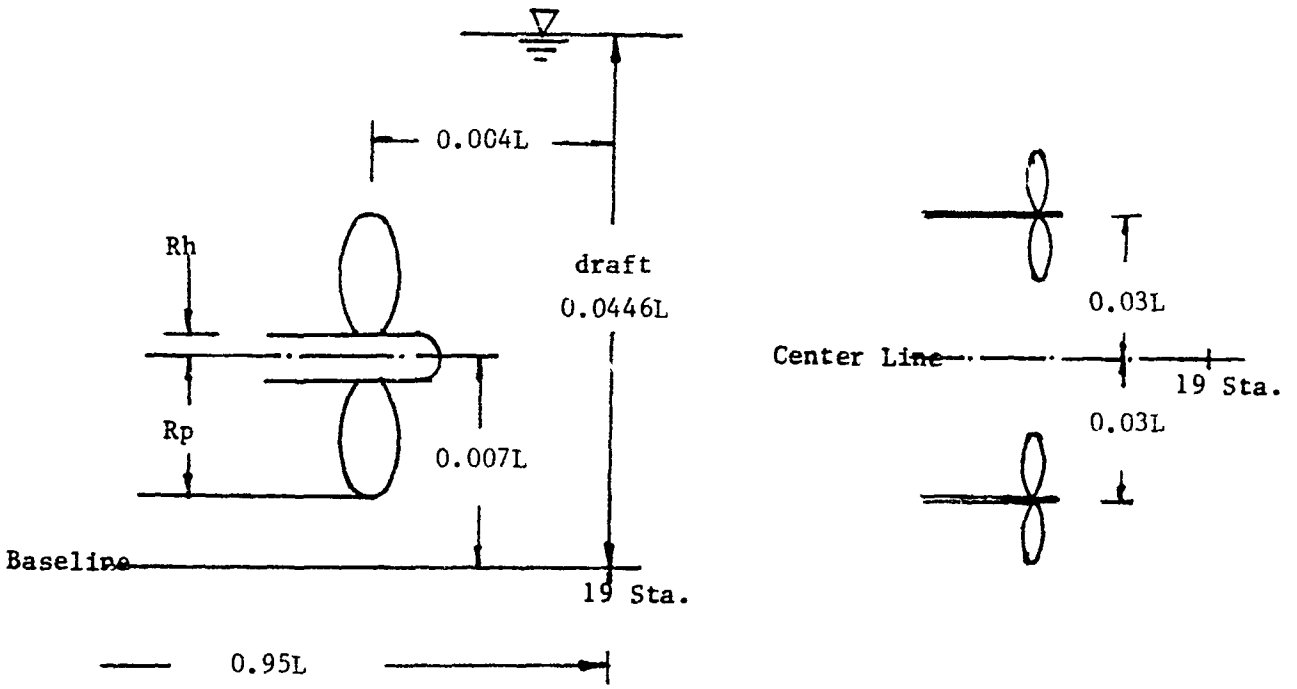

Figure 3. Propeller Location and Dimension

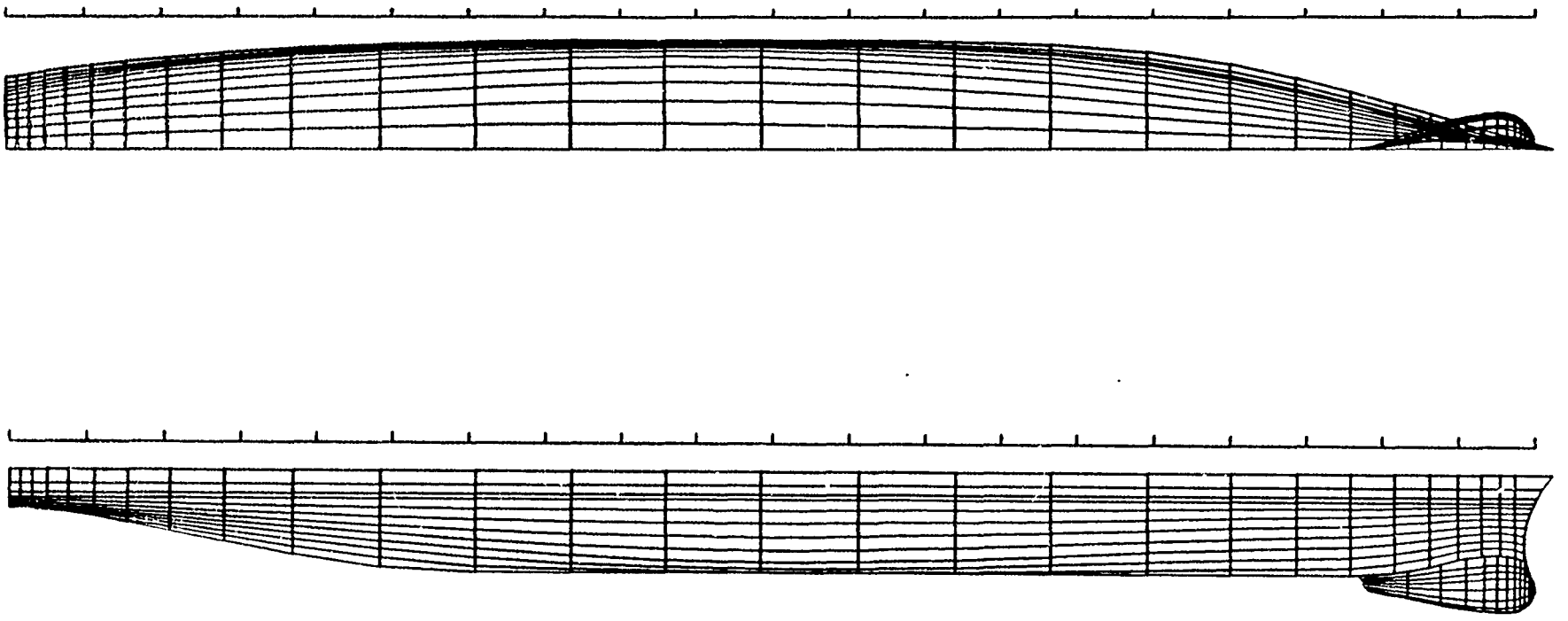

Figure 4. Ship Hull Panel Network

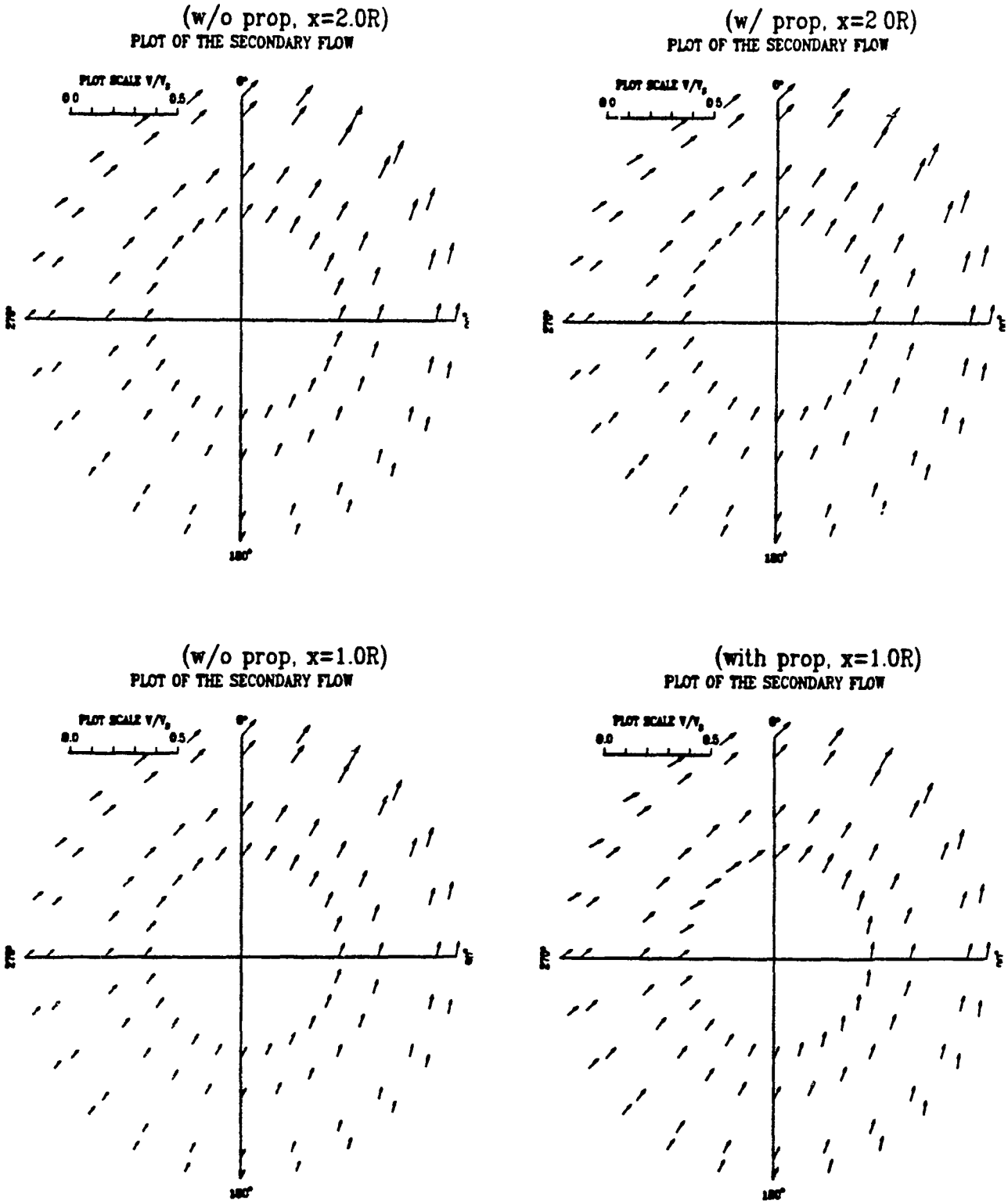

Figure 5 - Comparisons of Cross Flow Velocity Vectors with and without an Actuator Disk

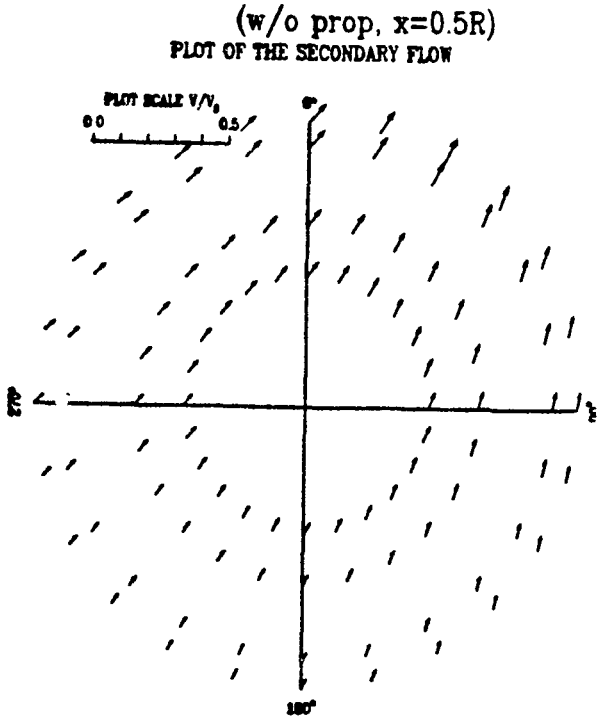

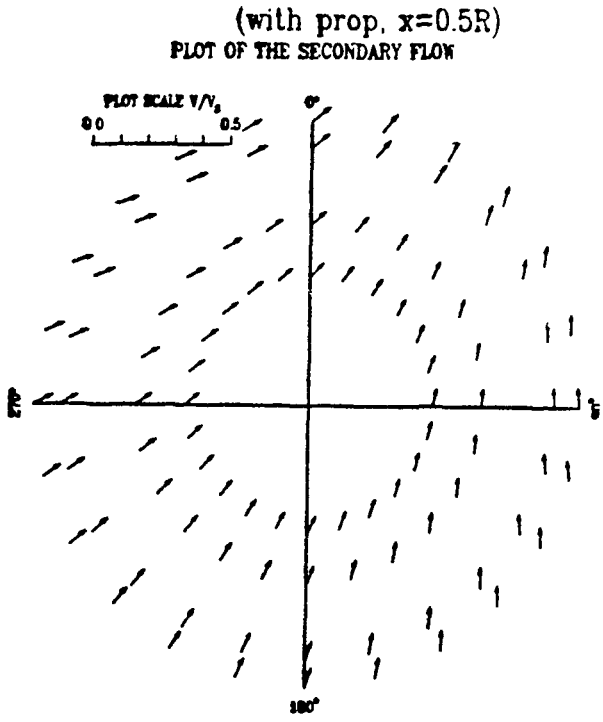

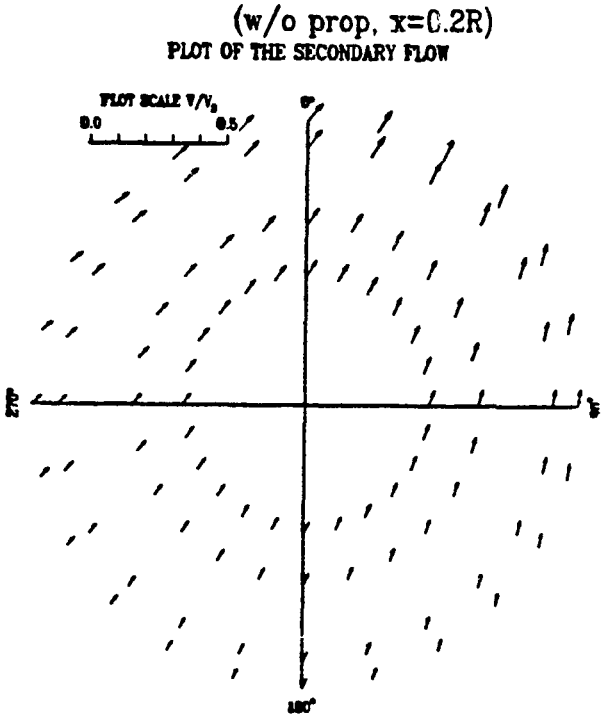

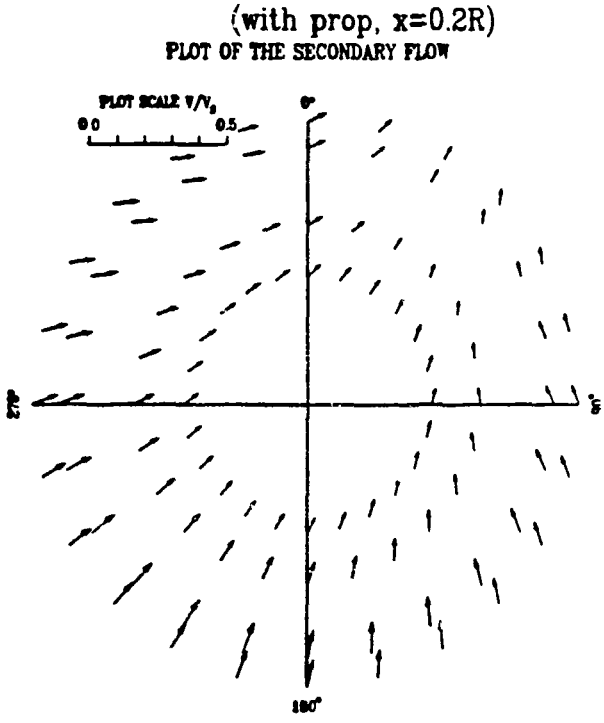

Figure 5 - continued

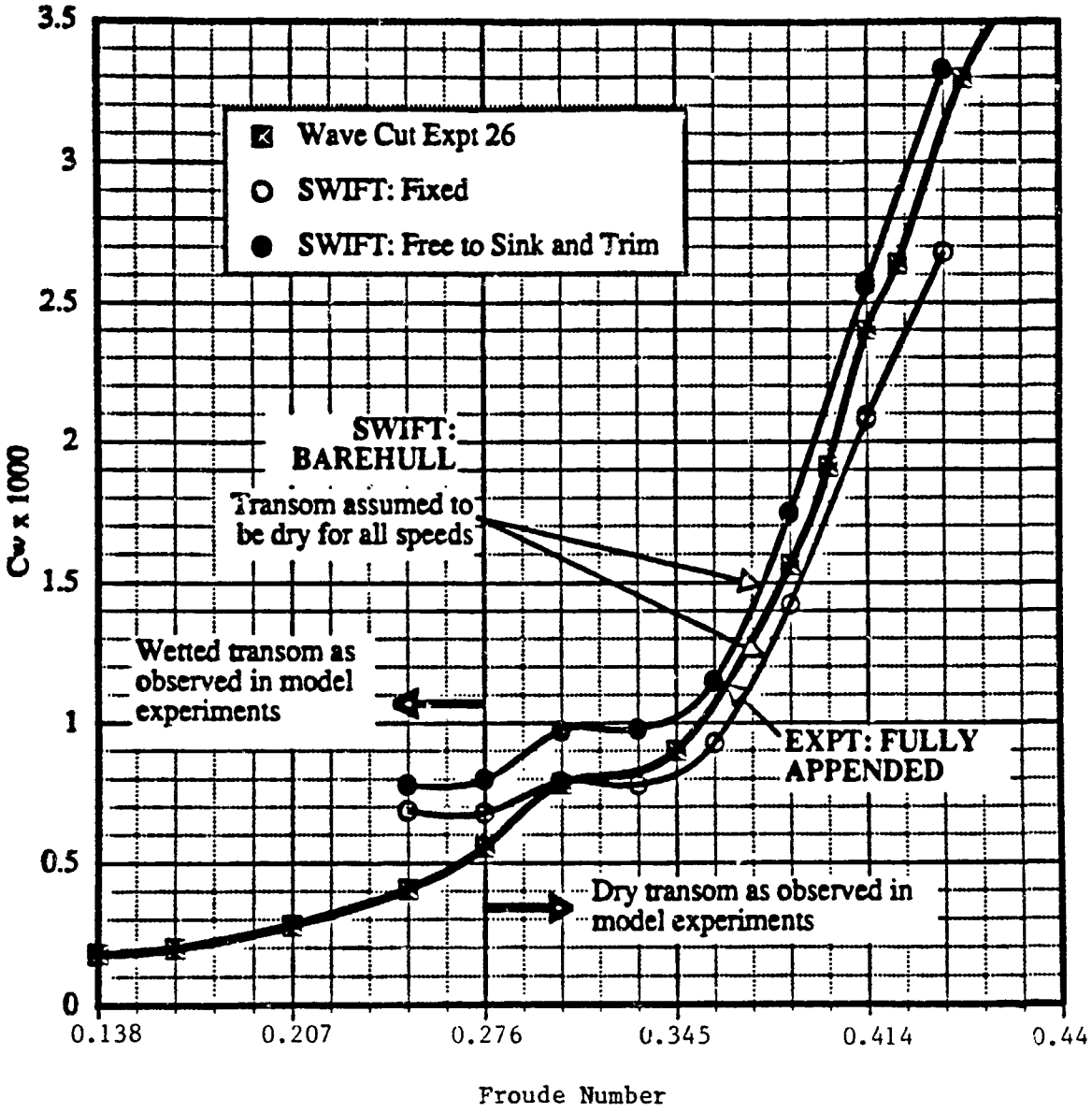

Figure 6. Comparison of Wave-Making Resistance Coefficients Predicted by SWIFT and from Model Experiments

Table 1 Ship Particulars	
B(beam)/L(hull length)	0.1266
D(draft)/B	0.3525
Dome Length/L	0.1137
Block Coeff.	0.5092
Wetted Surface Area Coeff.	0.6735
Waterplane Area Coeff.	0.7878
Transom Stern Area Coeff.	0.0619

where Block Coeff. = Volume/(L*B*D)
Wetted Surface Area Coeff. = Area/(L*(B+2D))
Waterpalne Area Coeff. = Area/(L*B)
Transom Stern Area Coeff. = Area/(B*D)

Table 2. Mean Axial and Total Velocity Increment due to Actuator Disk at F_n = 0.0.4140

Section at X=	Without Propeller		With Propeller		Velocity Increment(%)	
	|Vx|	|V|	|Vx|	|V|	Δ|Vx|	Δ|V|
-0.8188	0.97909	0.98200	0.99213	0.99542	1.33	1.37
-0.8553	0.97459	0.97694	0.99801	1.00088	2.40	2.45
-0.8735	0.97257	0.97464	1.00954	1.01227	3.80	3.86
-0.8845	0.97144	0.97332	1.02471	1.02778	5.48	5.60

where $|V| = \mathrm{sqrt}(Vx^2 + Vy^2 + Vz^2)$ and the propeller is located at x = -0.89178.

Table 3. Potential Fraction of Thrust Deduction

Fn	C_{TH} Eq.(15)	w_E	q Eq.(14)	Double Body Resistance Coefficient (x10^3)				Thrust Deduction Fraction		Ratio(%)
				C_R^{db} w/o prop	C_R^{db} w/ prop	ΔC_R^{db}	$\Delta \tilde{C}_R^{db}$	t_p Eq.(23)	t (Exp)	t_p/t
0.2760	0.3186	0.03	-0.15227	0.10452	0.21617	0.11165	15.538	0.04877	0.095	51.34
0.3447	0.3466	0.04	-0.16614	0.10452	0.22642	0.12190	16.964	0.04895	0.095	51.53
0.4140	0.4828	0.025	-0.22226	0.10452	0.26801	0.16349	22.752	0.04713	0.085	55.45
0.4400	0.5395	0.01	-0.24272	0.10452	0.28323	0.17871	24.870	0.04610	0.070	65.86

where

$$C_R^{db} = \frac{R}{\frac{1}{2}\rho U^2 S}$$

$$\Delta C_R^{db} = (C_R^{db})_{W/\,Prop} - (C_R^{db})_{W/O\,Prop}$$

$$\Delta \tilde{C}_R^{db} = \frac{\Delta R}{\frac{1}{2}\rho U^2 A_o} = \frac{\Delta C_R^{db} \cdot \frac{1}{2}\rho U^2 S}{\frac{1}{2}\rho U^2 A_o} = \frac{\Delta C_R^{db} \cdot S}{A_o}$$

in which S is the wetted surface area and A_O the projected propeller area.

Table 4. Free Surface Wave Fraction of Thrust Deduction

Fn	C_{TH} Eq.(15)	w_E	q Eq.(14)	Free Surface Resistance Coefficient ($\times 10^3$)				Thrust Deduction Fraction		Ratio(%) t_w/t
				$C_R^{h,w}$ w/o prop	$C_R^{h,w}$ w/ prop	$\Delta C_R^{h,w}$	$\Delta \tilde{C}_R^{h,w}$	t_w Eq.(24)	t (Exp)	
0.2760	0.3186	0.03	-0.15227	0.57490	0.63984	0.06494	9.0372	0.02837	0.095	29.86
0.3447	0.3466	0.04	-0.16614	0.70712	0.77898	0.07196	10.014	0.02885	0.095	30.37
0.4140	0.4828	0.025	-0.22226	1.97528	2.04809	0.07281	10.132	0.02099	0.085	24.69
0.4400	0.5395	0.01	-0.24272	2.55388	2.62477	0.07089	9.8652	0.01829	0.070	26.13

where

$$C_R^{h,w} = \frac{R}{\frac{1}{2}\rho U^2 S}$$

$$\Delta C_R^{h,w} = (C_R^{h,w})_{W/\ Prop} - (C_R^{h,w})_{W/O\ Prop}$$

$$\Delta \tilde{C}_R^{h,w} = \frac{\Delta R}{\frac{1}{2}\rho U^2 A_o} = \frac{\Delta C_R^{h,w} \cdot \frac{1}{2}\rho U^2 S}{\frac{1}{2}\rho U^2 A_o} = \frac{\Delta C_R^{h,w} \cdot S}{A_o}$$

in which S is the wetted surface area and A_O the projected propeller area.

Table 5. Thrunst Deduction Comparison between Experiment and Computation

Fn	C_{TH} (Exp)	w_E (Exp)	Thrust Deduction Fraction				Ratio (%)
			Computation			Experiment	
			t_p	t_w	$t_p + t_w$	t	$(t_p+t_w)/t$
0.2760	0.3186	0.03	0.04877	0.02837	0.07714	0.095	81.20
0.3447	0.3466	0.04	0.04895	0.02885	0.07780	0.095	81.90
0.4140	0.4828	0.025	0.04713	0.02099	0.06812	0.085	80.14
0.4400	0.5395	0.01	0.04610	0.01829	0.06439	0.070	91.99

REFERENCES

[1] Dickmann, H.E., " Thrust Deduction, Wave Resistance of a Propeller, and Interaction with Ship Waves (in German)," Ingenieur Archiv 9, 452-486, 1938

[2] Nowacki, H., and Sharma, S.D., " Free Surface Effects in Hull Propeller Interaction," The University of Michigan , College of Engineering Report 112, September, 1971

[3] Beveridge, J.L., " Thrust Deduction in Contrarotating Propellers," NSRDC Rep. 4332, Nov., 1974

[4] Stern, F., Kim, H.T., Patel, V.C., and Chen, H.C.," Viscous-Flow Computation of Propeller-Hull Interaction," Proc. of the 16th Symp. on Naval Hydrodynamics, UC Berkeley, CA, 1986, pp 246-267.

[5] Yamazaki, R., and Nakatake, K., " Free-Surface Effect on the Hull-Propeller Interaction," Proc. of the 15th Symp. on Naval Hydrodynamics, Hamburg, Germany, Sept., 1984

[6] Dawson, C.W., "A Practical Computer Methods for Solving Ship-Wave Problem," Proc.of the 2nd International Conference on Numerical Ship Hydrodynamics, Berkeley, Calif., 1977

[7] Kim, Y.H., Kim, S.H., and Lucas, T., " Advanced Panel Method for Ship Wave Inviscid Flow Theory(SWIFT)," DTRC-89/029, Nov., 1989